LC-polyimides: 5. Poly(ester-imide)s derived from *N*-(4-carboxyphenyl) trimellitimide and α,ω-dihydroxyalkanes

Hans R. Kricheldorf and Gert Schwarz
University Institute for Technical and Macromolecular Chemistry, Bundesstrasse 45, D-2000 Hamburg 13, FRG

and Javier de Abajo and José G. de la Campa
Institute of Polymer Science and Technology, Calle Juan de la Cierva, E-28006 Madrid, Spain
(Received 16 March 1990; accepted 12 April 1990)

N-(4-carboxyphenyl)trimellitimide was prepared from trimellitic anhydride and 4-aminobenzoic acid and esterified with methanol. Transesterification with α,ω-dihydroxyalkanes in the melt yielded a series of poly(ester-imide)s with varying spacer lengths. These poly(ester-imide)s were characterized by elemental analyses, inherent viscosities, differential scanning calorimetry measurements, wide angle X-ray spectroscopy powder and fibre patterns, including synchrotron radiation measurements at variable temperature, optical microscopy with polarized light, and thermogravimetric analyses. Poly(ester-imide)s with even-numbered spacers can form three different kinds of solid phase, including a smectic glass and a crystalline smectic phase. Fibre patterns of melt-spun fibres indicate a high degree of order for series of subsequent layers, even when any order inside the layers is lacking. Poly(ester-imide)s with odd-numbered spacers crystallize much more slowly and can be quenched from the isotropic melt, so that isotropic glasses can be obtained.

(Keywords: LC-polyimides; characterization; synthesis)

INTRODUCTION

The present work is part of a broader study on the synthesis and characterization of thermotropic poly(ester-imide)s. In the first paper of this series[1] the poly(ester-imide)s *1a–i* were described. It was demonstrated that the aromatic imide unit of these polyesters is a better mesogen than 4,4'-dihydroxybiphenyl. The present work was aimed at studying the isomeric poly(ester-imide)s *2a–h*. A comparison of isomeric poly(ester-imide)s *1a–i* and *2a–h* is of interest, because it was recently demonstrated[2] that isomeric fully aromatic copoly(ester-imide)s possess different properties. See *Formula A*.

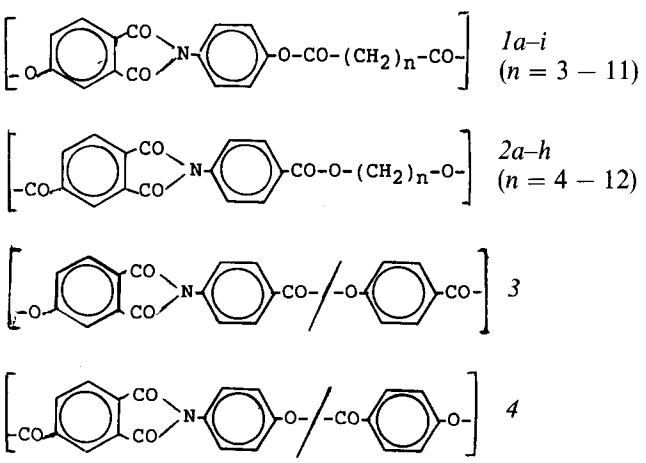

Formula A

0032-3861/91/050942-08

EXPERIMENTAL

Materials

Trimellitic anhydride was a gift from Bayer AG (4150-Krefeld, FRG). It was purified by recrystallization from toluene containing acetic anhydride. 4-Aminobenzoic acid was also a gift from Bayer AG, but it was used without purification. α,ω-Dihydroxyalkanes were purchased from Aldrich Co. (St Louis, MO, USA). They were purified by azeotropic drying with toluene and subsequent fractionation in vacuum.

Dimethylester of N-(4-carboxyphenyl)trimellitimide

N-(4-carboxyphenyl)trimellitimide[3,4] (0.5 mol) was refluxed in 1 l of dry methanol containing 1 ml of concentrated sulphuric acid. After 4 h the reaction mixture was concentrated, diluted with dichloromethane, washed several times with water and dried over Na_2SO_4. The dichloromethane solution was concentrated and the residue crystallized from hot toluene. Yield: 70%; m.p. 204°C. Analyses: calculated for $C_{18}H_{13}NO_6$(339.32): C, 63.71; H, 3.87; N, 4.13; found: C, 63.41; H, 3.91; N, 4.02.

Polycondensations (see Table 1)

The dimethylester *6* (50 mmol), an α,ω-diol (50 mmol) and titanium tetraisopropoxide were weighed into a cylindrical glass reactor equipped with mechanical stirrer and gas inlet and outlet tubes. The reaction mixture was stirred for 2 h at 190–200°C under a slow stream of nitrogen, whereby most methanol was distilled off. An excess of diol (see *Table 1*) was then added and the

Table 1 Yields and properties of poly(ester-imide)s *2a–2h*

Polymer formula	α,ω-Diol: *n*	α,ω-Diol: Molar excess	Yields (%)	η_{inh} (dl g^{-1})	Elemental formula (Formula weight)	Elemental analyses	C	H	N	T_g[a] (°C)	T_{m_1}[a] (°C)	T_{m_2}[a] (°C)
2a	4	120%	77	0.43[b]	$C_{20}H_{15}NO_6$ (365.33)	Calc.	65.75	4.11	3.84	94	229	240
						Found	64.99	4.30	3.30			
2b	5	120%	92	0.35[b]	$C_{21}H_{17}NO_6$ (379.36)	Calc.	66.49	4.49	3.69	89	127	175
						Found	65.59	4.67	3.62			
2c	6	10%	88	0.52[b]	$C_{22}H_{19}NO_6$ (393.38)	Calc.	67.17	4.83	3.56	82	203	223
						Found	67.11	4.93	3.65			
2d	7	10%	92	0.57[b]	$C_{23}H_{21}NO_6$ (407.41)	Calc.	67.81	5.16	3.44	79	123	164
						Found	67.97	5.14	2.99			
2e	8	8%	84	0.78[c]	$C_{24}H_{23}NO_6$ (421.43)	Calc.	68.41	5.46	3.33	75	177	196
						Found	67.93	5.57	2.98			
2f	9	5%	81	0.55[b]	$C_{25}H_{25}NO_6$ (435.46)	Calc.	68.96	5.79	3.23	55	111	161
						Found	68.59	5.94	2.98			
2g	10	5%	95	0.91[c]	$C_{26}H_{27}NO_6$ (449.49)	Calc.	69.49	6.01	3.12	59	123	171
						Found	68.85	5.91	2.74			
2h	12	5%	95	0.72[c]	$C_{28}H_{31}NO_6$ (477.60)	Calc.	70.44	6.50	2.94	44	122	158
						Found	70.13	6.65	2.99			

[a] From d.s.c. measurements with a heating rate of 20°C min^{-1}. Depending on the thermal history these values vary within the limits ± 2°C
[b] Measured with $c = 2$ g l^{-1} at 20°C in *N*-methylpyrrolidone
[c] Measured with $c = 2$ g l^{-1} at 20°C in CH_2Cl_2/TFA (4:1 by volume)

temperature was gradually raised to 260–270°C over a period of 4 h. During the last 30 min a vacuum of ≈ 0.5 bar (50 kPa) was applied. The highly viscous melt thus formed solidified upon cooling. It was dissolved in a mixture of dichloromethane and trifluoroacetic acid (4:1 by volume) and precipitated with cold acetone. After intensive washing with acetone the poly(ester-imide) was dried at 50–55°C in vacuum.

Measurements

The viscosities were measured with an automated Ubbelohde viscometer thermostated at 25°C.

The differential scanning calorimetry (d.s.c.) measurements were made with a Perkin–Elmer DSC-4 in aluminium pans at a heating or cooling rate of 20°C min^{-1}. The wide angle X-ray scattering (WAXS) powder patterns were obtained on a Siemens D-500 powder diffractometer at 25°C by means of Ni-filtered Cu-K_α radiation. The synchrotron radiation measurements ($\lambda = 1.50$ Å) (1 Å = 10^{-1} nm) were made at HASYLAB-DESY (Hamburg, FRG)[5] at a heating rate of 20°C min^{-1} in vacuum.

The fibres were spun from poly(ester-imide)s molten at 280–290°C by means of a home-made mini-extruder.

RESULTS AND DISCUSSION

Syntheses

All poly(ester-imide)s in this work were prepared by the same synthetic approach. *N*-(4-carboxyphenyl) trimellitimide (*5*) was prepared, and the free carboxyl group was then esterified with methanol in the presence of concentrated sulphuric acid (Equations (1)–(3)). See *Formula B*.

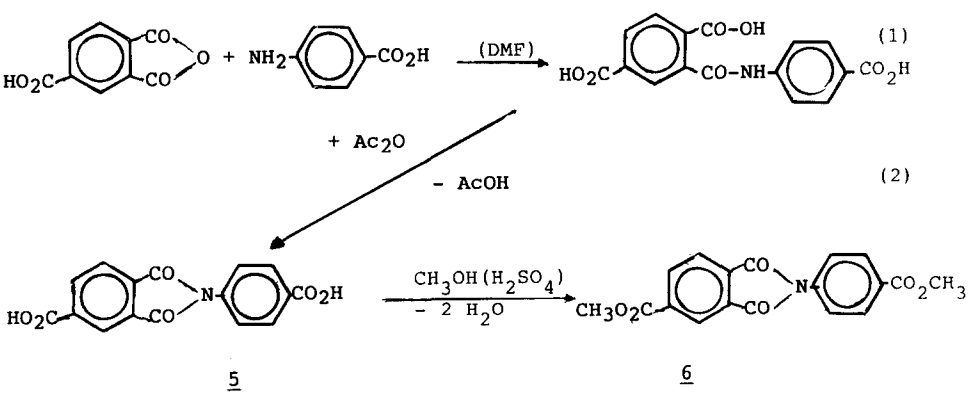

5 6

Formula B

The resulting diester 6 was finally polycondensed with various α,ω-dihydroxyalkanes in the presence of $Ti(OBu)_4$ as transesterification catalyst. All polycondensations were conducted in the melt at temperatures up to 260 (*2a–d*) or 270°C (*2d–h*). To compensate for the loss of volatile diols, an excess of diol was used. This excess of diol, yields, inherent viscosities and elemental analyses are summarized in *Table 1*. Absolute molecular weights were not measured, because all poly(ester-imide)s were insoluble in aprotic organic solvents. None the less, all samples with $\eta_{inh} > 0.5$ dl g^{-1} allowed spinning of fibres from the molten state.

Properties of even-numbered poly(ester-imide)s

A detailed study of phase transitions revealed that poly(ester-imide)s with an even number of methylene groups (*2a, c, e, g, k*) and those with an odd number (*2b, d, f*) show significant differences. Therefore, the properties of the two groups will be discussed separately. When samples with even-numbered spacers were subjected to d.s.c. measurements with a heating and cooling rate of 20°C min^{-1}, a weak glass transition step and two endotherms were found in the first heating trace. Samples exhibiting these characteristics (*Figure 1A*) were precipitated with acetone and dried at 50–55°C in a vacuum. The two endotherms are denoted T_{m_1} and T_{m_2} (*Table 1*). As discussed below in connection with WAXS patterns, these endotherms represent in the case of *2c, e, g, h* the melting processes of two crystal modifications (denoted I and II). In the case of *2a* only one modification (probably II) was detectable and the existence of two closely neighbouring endotherms obviously indicates crystallites of different size and perfection in analogy with most semicrystalline polymers.

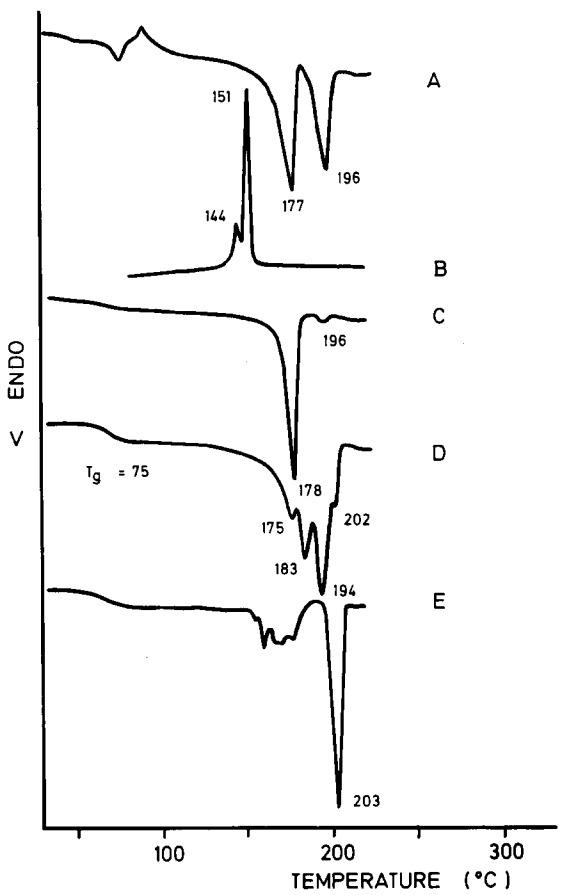

Figure 1 D.s.c. measurements (heating and cooling rate 20°C min^{-1}) of poly(ester-imide) *2e* ($n = 8$): A, first heating after drying at 50–55°C; B, first cooling; C, second heating; D, first heating after annealing at 0.5 h, 185°C; E, first heating after annealing 14 h, 185°C

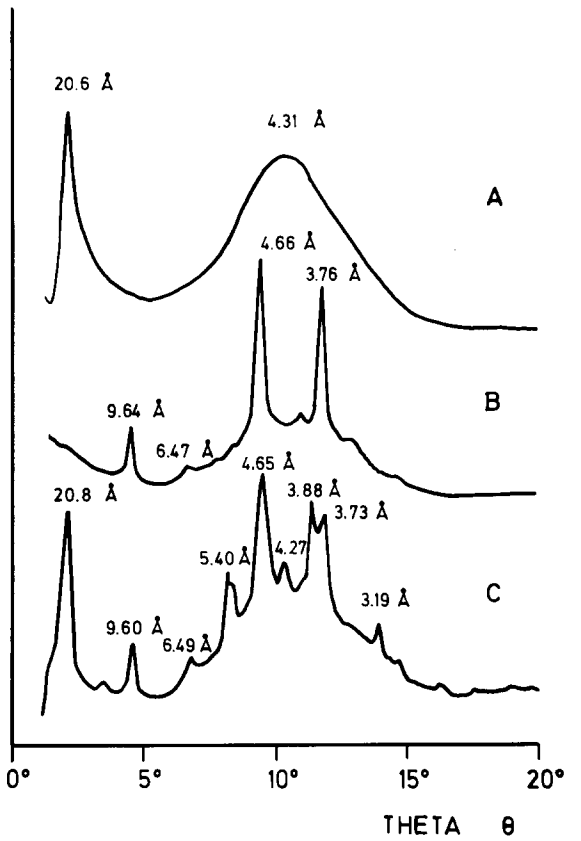

Figure 2 WAXS powder patterns of *2c* ($n = 6$) measured at 25°C: A, after quenching from the isotropic melt; B, annealed for 16 h, 160°C; C, annealed for 16 h, 215°C

When several heating and cooling cycles were repeated, only one endotherm and one exotherm were reproducible in the heating and cooling traces of *2a*, *c* and *e* (*Figure 1B, C*). This endotherm corresponds to T_{m_1} in the first heating trace. Thus cooling from the melt followed by slow heating above T_g or by annealing between T_g and T_{m_1} yielded nearly pure modifications I in the case of *2c* and *e* (*Figures 2B* and *3B*). However, the same procedure always yielded mixtures of modifications I and II, when applied to *2g* and *h*. Therefore, pure modifications I of *2g* or *2h* were never obtained. Annealing of *2a, c, e, g*, and *h* at temperatures between T_{m_1} and T_{m_2} led to the disappearance of T_{m_1} and heating traces displaying a glass transition step and the endotherm of T_{m_2} were obtained (*Figure 1D, E*).

Optical microscopy revealed for all even and odd-membered poly(ester-imide)s an isotropic melt above T_{m_2}. For *2c* and *e* an isotropic melt was also found above T_{m_1}. Annealing of these melts 10–15°C above T_{m_1} resulted in gradual formation of new crystallites, which melt upon heating above T_{m_2} in good agreement with the d.s.c. measurements.

The WAXS powder patterns of modifications II of all even-membered poly(ester-imide)s have two features in common: numerous sharp reflections for $2.5 \leqslant \theta \leqslant 15°$ and one intensive reflection for $1.5 \leqslant \theta \leqslant 2.5°$ (*Figures*

Table 2 Atomic distances (Å) and relative intensities[a] of X-ray powder reflections of modification II

2a	18.2(v.s.)	12.3(v.w.)	5.39(s)	4.84(w)	3.95(s)	3.22(w)	2.77(v.w.)			
2b	17.1(v.s.)	5.43(s)	4.62(w)	3.93(s)	3.38(w)	2.78(v.w.)				
2c	20.8(v.s.)	12.5(v.w.) 3.04(v.w.)	9.60(s) 2.75(w)	6.49(w)	5.40(s)	4.65(v.s.)	4.27(w)	3.88(s)	3.73(s)	3.19(w)
2d	19.2(v.s.)	13.6(v.w.)	5.35(s)	4.81(w)	3.90(s)	3.21(w)	2.74(v.w.)			
2e	21.8(v.s.)	8.26(v.w.) 2.85(v.w.)	6.96(v.w.)	5.98(w)	5.46(w)	4.76(w)	4.41(w)	4.02(s)	3.40(s)	3.31(w)
2f	22.6(v.s.)	14.0(v.w.)	5.37(s)	4.62(s)	4.52(s)	3.93(s)	3.48(v.w.)	3.22(w)	2.75(w)	
2g	25.2(v.s.)	4.44(v.s.)								
2h	26.7(v.s.)									

[a] V.s., very strong; s, strong; w, weak; v.w., very weak

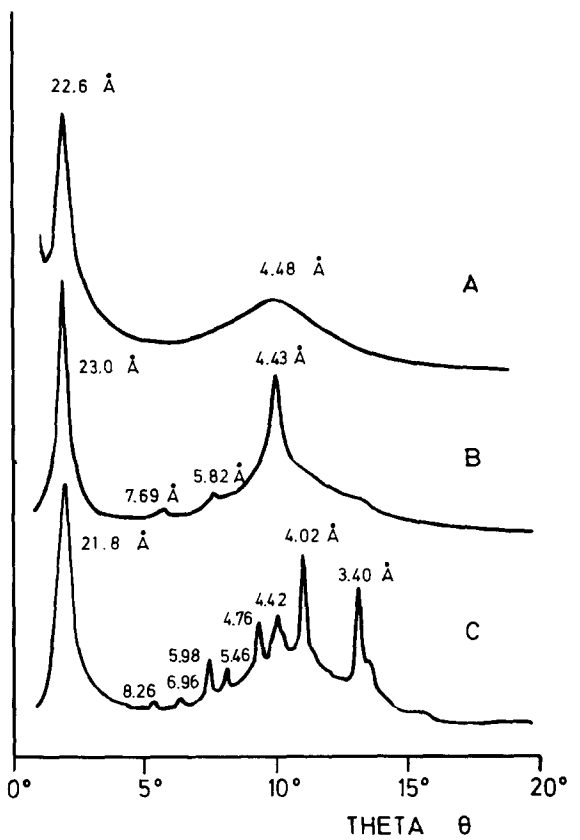

Figure 3 WAXS powder pattern of *2e* ($n = 8$) measured at 25°C: A, after quenching; B, annealed for 16 h, 160°C; C, annealed for 16 h, 185°C

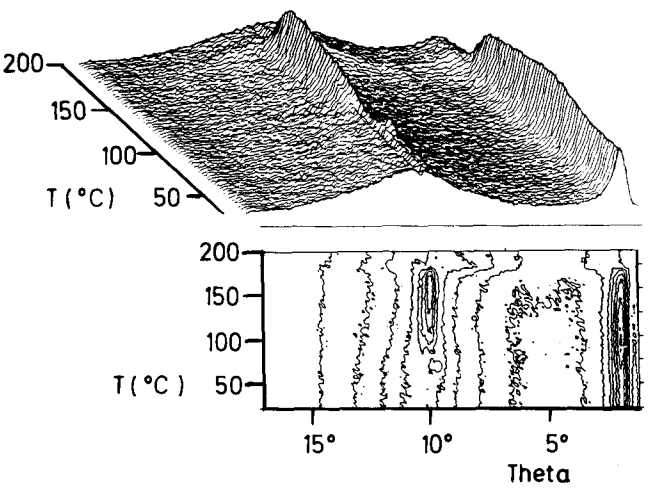

Figure 4 WAXS powder patterns of *2e* quenched from the melt. Measurements were conducted with synchrotron ra. (irradiation: 10 s) at a heating rate of 20°C min^{-1}

2C and *3C*). All these reflections are listed in *Table 2*. As discussed below in more detail, the intensive small angle reflection indicates a layered supermolecular structure, and the numerous reflections above $\theta = 2.5°$ suggest that these crystalline smectic structures do not possess a hexagonal chain packing (e.g. smectic E or H).

The WAXS patterns of modifications I of *2c* and *e* not only differ largely from those of modifications II, they also differ from each other (*Figures 2B* and *3B*). In contrast to *2e* the small angle reflection is absent in the WAXS pattern of *2c*. Interestingly, an intensive small angle reflection is detectable in all WAXS patterns of glassy materials obtained by rapid cooling of the isotropic melts (*Figures 2A* and *3A*). Hence, the formation of a layer structure upon cooling must be kinetically more favourable than perfection of the lateral and conformational order of the mesogens. This result is conceivable considering the high polarity of the mesogens, on the one hand, and their low degree of symmetry, on the other hand.

Heating of a smectic glass above T_g is in principle expected to bring about a mobile mesophase such as smectic A or C. But such a mobile mesophase was never detectable by microscopy. The reason for this failure was elucidated by WAXS measurements conducted with synchrotron radiation at a heating rate of 20°C min^{-1}. As illustrated by *Figure 4* heating glassy *2e* above T_g results in gradual crystallization. When the melting point of modification I is reached all reflections disappear. Thus optical microscopy, d.s.c. and WAXS measurements are in perfect agreement.

In this connection it is worth mentioning that the small angle reflections of glassy state and modification II did not show any systematic deviation. Only a slight scattering of the θ values depending on the thermal history of the samples was observed. This result means that the distances between the layer planes are nearly identical for both glassy and crystalline states.

Properties of odd-membered poly(ester-imide)s

D.s.c. measurements of *2b* ($n = 5$) and *2d* ($n = 7$) made at a heating (and cooling) rate of 20°C min^{-1} gave the following results. The samples dried at 50–55°C display in addition to a glass transition step only one broad endotherm representing the melting process of modification II (*Figure 5A*). Cooling and reheating produced

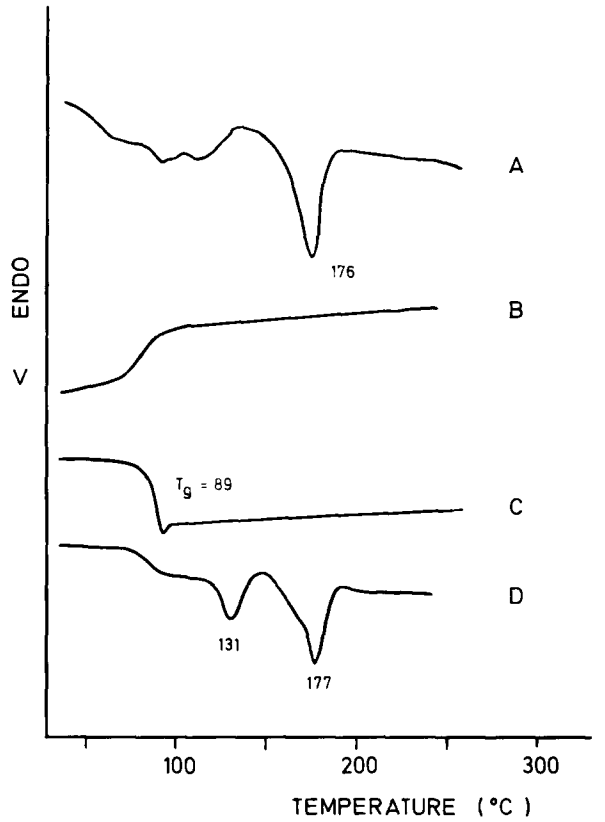

Figure 5 D.s.c. measurements (heating and cooling rate 20°C min^{-1}) of poly(ester-imide) *2b*: A, first heating after drying at 50–55°C; B, first cooling; C, second heating; D, first heating after annealing for 16 h at 100°C

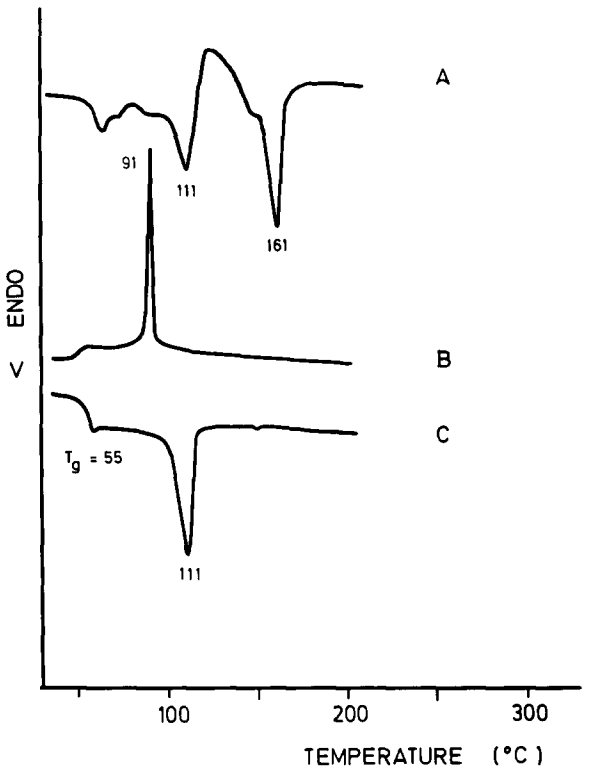

Figure 6 D.s.c. measurements (heating and cooling rate 20°C min^{-1}) of poly(ester-imide) *2f* (n = 9): A, first heating after drying at 50–55°C; B, first cooling; C, second heating

neither an exotherm nor an endotherm (*Figure 5B, C*). Thus in contrast to the even-membered poly(ester-imide)s a normal isotropic glassy state could be obtained for *2b* and *2d*. Annealing of the original samples around or below 100°C provided d.s.c. heating traces with two endotherms (T_{m_1} and T_{m_2}, *Figure 5D*). Annealing below or above T_{m_1} never yielded a pure modification I. However, in both cases (*2b* and *2d*) semicrystalline materials with pure modification II were obtained by long annealing (12 h) 15–20°C below T_{m_2}. Furthermore, a semicrystalline material containing pure modification I resulted upon spinning fibres of *2d* from the isotropic melt.

Still more complex properties were found in the case of *2f* (n = 9). The first heating trace exhibits two endotherms in analogy with those of even-membered poly(ester-imide)s (*Figure 6* and *1*). In contrast to *2b* and *2d* the cooling trace displays a strong exotherm, indicating a rapid crystallization process due to higher segmental mobility. Again in agreement with even-membered species (e.g. *2c, e*), one endotherm, representing the melting of modification I, is observable in the second heating trace (*Figure 6C*). In contrast to all other poly(ester-imide)s of this work, annealing between 80 and 100°C produces heating traces with three endotherms (*Figure 7A, B*). The intensities of all three endotherms depend largely on annealing time and temperature. It remained unclear whether the new endotherm at 146 ± 1°C indicates a third modification, because a sample exclusively showing this endotherm was never obtained. Annealing at 150°C produces a semicrystalline material with one endotherm at 162 ± 1°C (*Figure 7C*). By comparison of d.s.c. traces

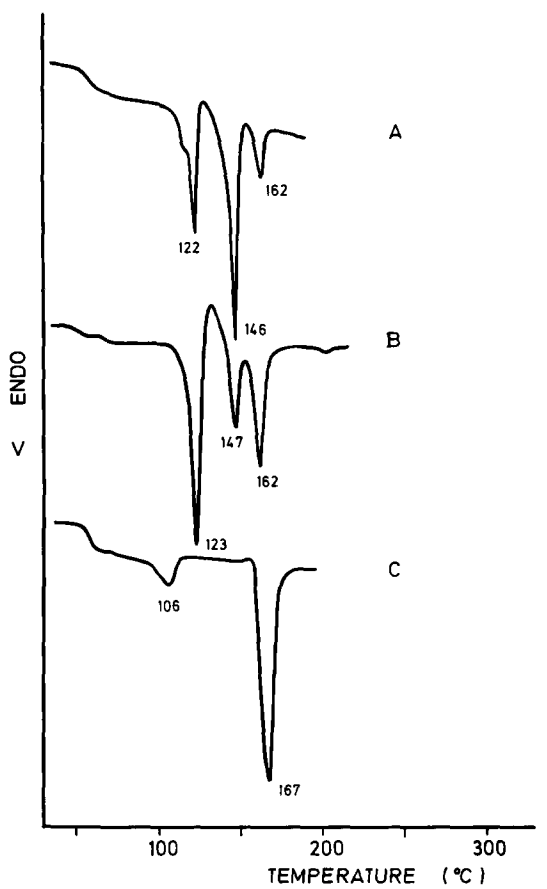

Figure 7 D.s.c. measurements (first heating traces only) of poly(ester-imide) *2f* (n = 9): A, after annealing for 1 h, 100°C; B, after annealing for 70 h, 100°C; C, after annealing for 16 h, 150°C

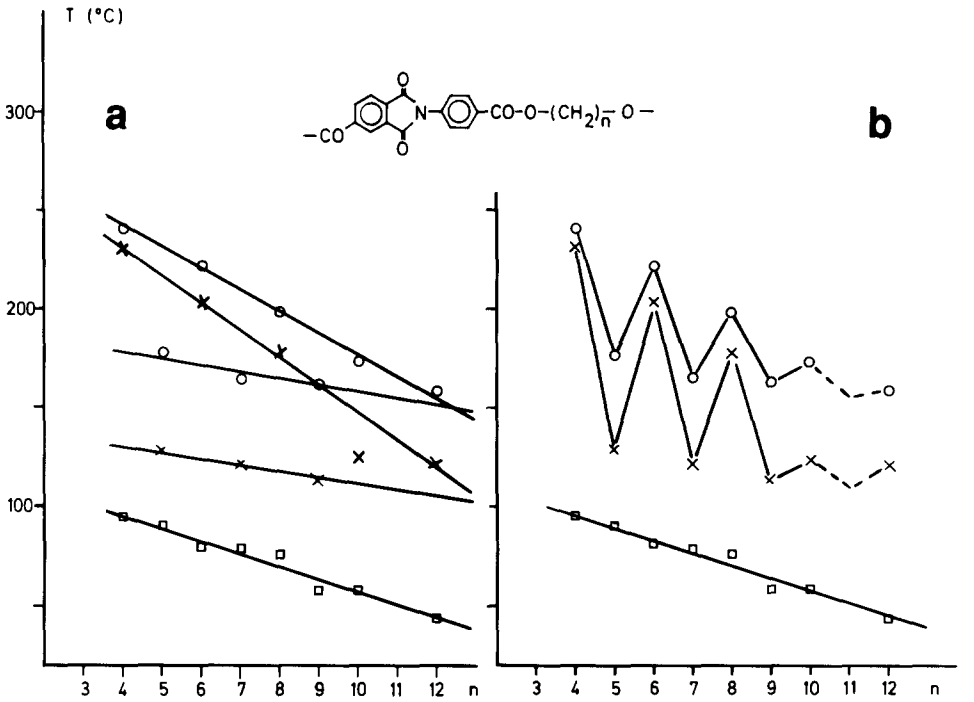

Figure 8 Plot of glass transition temperatures, T_g (□) and melting points, T_{m_1} (×) and T_{m_2} (○) *versus* number of CH_2 groups in *2a–i*

and WAXS measurements of *2f* with *2b* and *d* this 'high temperature' endotherm is attributed to the melting of modification II. A plot of endotherm *versus* spacer lengths (*Figure 8a*) illustrates this assignment and demonstrates that the structure/property relationships for even and odd-membered poly(ester-imide)s differ significantly. The plot of *Figure 8b* also displays a strong odd–even effect for the melting points of *2a–h* in close analogy to other 'semi-rigid' poly(ester-imide)s *7a–i*, derived from trimellitic acid[6]. See *Formula C*.

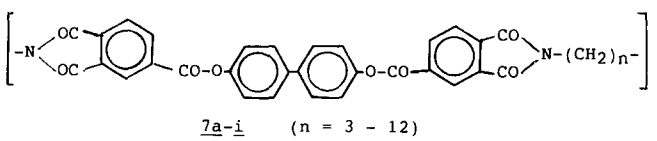

Formula C

Fibre patterns of poly(ester-imide)s 2a–h

The molecular weights of poly(ester-imide)s *2a*, *c*, *e*, *g*, and *h* proved to be high enough to allow spinning of long (several metres) fibres from the melt at 280–300°C. However, before this spinning process thermogravimetric analyses were conducted in air with a heating rate of 10°C min^{-1}. The thermogravimetric analysis (t.g.a.) curves of *2a–h* have in common that thermal degradation (1–2% loss of weight) begins in the temperature range 350–370°C. As demonstrated by *Figure 9*, a rapid degradation only occurs above 400°C. A similar thermostability was found for poly(ester-imide)s *7a–i*[6]. From these measurements it is obvious that neither the spinning of fibres nor the phase transitions discussed above were affected by thermal degradation.

The fibre patterns taken from fibres prepared at a spinning rate of 2 m s^{-1} exhibited two unexpected features. A series of seven or more sharp reflections were observable on the meridian, whereas only a broad diffuse

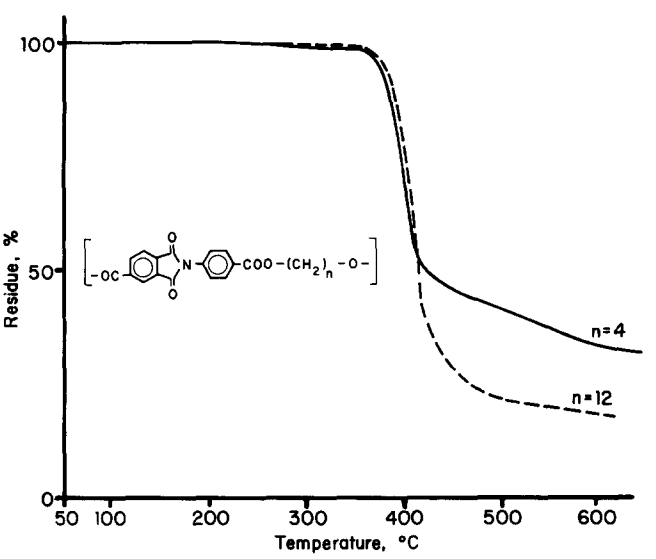

Figure 9 Thermogravimetric analyses of poly(ester-imides) *2a* and *2h* conducted at a heating rate of 10°C min^{-1} in air

reflection appears on the equator (*Figure 10*). A WAXS pattern measured along the fibre axis confirms the existence of a series of extremely sharp reflections (*Figure 11*). Evaluation of the atomic distances on the basis of the Bragg equation indicates that all sharp reflections represent the first and higher order reflections of the same layer structure.

The high degree of order along the fibre axis contrasts sharply with the complete disorder inside individual layers, as indicated by the diffuse reflections on the equator. In other words, these fibres possess the supermolecular structure of a smectic glass. Annealing of the fibres at 100°C generates sharp reflections on the equator, indicating that the repeating units now also have adopted a crystalline order inside the layer planes. This consequence confirms that a glassy state existed before

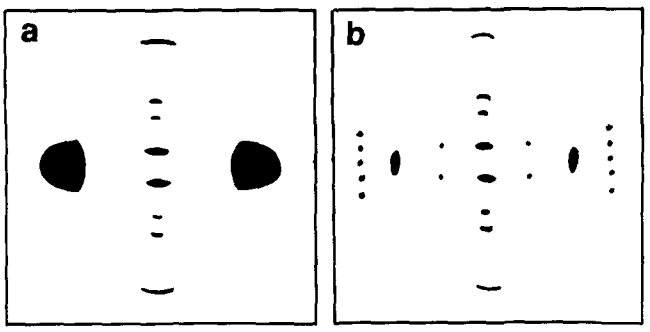

Figure 10 X-ray fibre patterns of poly(ester-imide) *2e*: (a), fibre as spun from the melt at 300°C; (b), after annealing for 16 h at 160°C

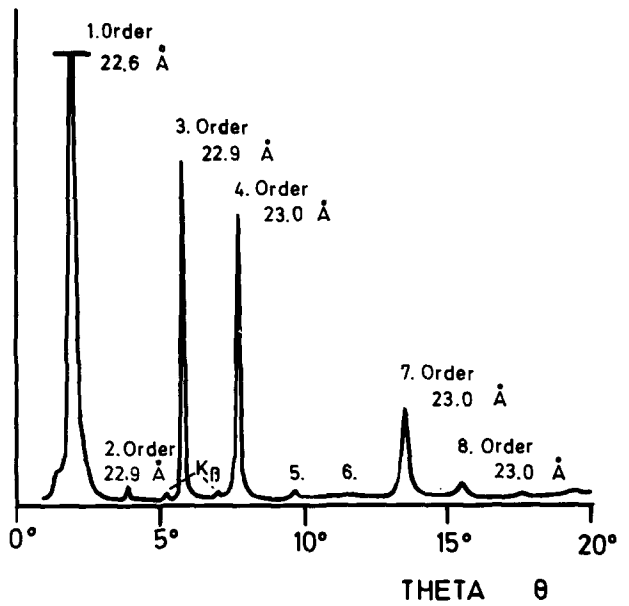

Figure 11 WAXS pattern of parallel fibres of *2e*: meridional reflections only

annealing. D.s.c. measurements of the annealed fibres yielded endotherms identical with T_{m_1} of powders *2a*, *b*, *c*, *d* and *e* or with T_{m_2} of powders *2f*, *g* and *h*. In agreement with the d.s.c. measurements, WAXS patterns of powdered, annealed fibres were almost identical with those of the original powders (e.g. *Figures 2* and *3*). These results confirm that the crystalline smectic state of the fibres is identical with modification I or II of crystalline powders.

Also, poly(ester-imide)s with odd-membered spacers (*2b*, *2d* and *2f*) allowed spinning of fibres from the isotropic melt. However, the fibre patterns of these materials were different from those of even-membered poly(ester-imide), because only the first-order small angle reflection was detectable. Obviously, the supermolecular layer structure is less perfectly arranged along the fibre axis than for even-membered spacers.

Owing to the higher overall order of annealed fibres, their small angle reflections were evaluated with regard to layer distances. The atomic distances calculated from the first order reflections by means of the Bragg equation were plotted against the number of methylene units in the spacers (*Figure 12*). This plot shows a good linear fit of all layer distances calculated for even-membered spacers and a similar linear relationship for odd-membered spacers. The linearity of these plots is amazing, because part of the samples exists in modification I and another part in modification II. The identical slope of both plots indicates that the even- and odd-membered spacers adopt identical tilt angles relative to the layer planes (α in the scheme of *Figure 13*). Assuming a planar zig-zag conformation of the aliphatic spacers and 2.53 Å for the 'pitch' of an ethylene unit, a tilt angle of $63 \pm 1°$ may be calculated in perfect agreement with layer structure found for poly(ester-imide)s *7a–i*.

Despite identical slopes, the layer distances of even- and odd-membered poly(ester-imide)s differ by approximately 2 Å (*Figure 12*). This difference obviously results from different tilt angles of the imide mesogens as indicated by β and β' in *Figure 13*. Assuming an extended spacer with $\alpha = 63 \pm 1°$, a tilt angle $\beta = 69°$ and $\beta' = 49 \pm 1°$

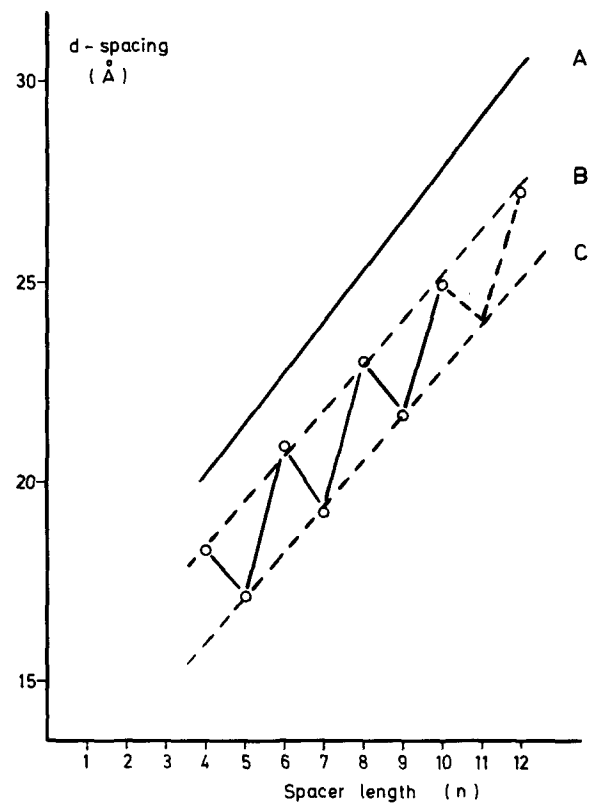

Figure 12 Plot of distances between neighbouring layer planes of modification I *versus* spacer lengths of *2a–i*: A, values calculated for extended repeating units perpendicular to layer planes; B, C, measured values

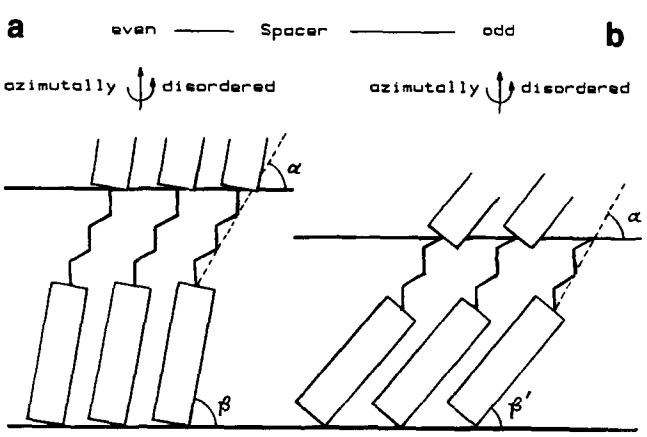

Figure 13 Schematic model of the supermolecular layer structure (modification I) of (a) even-membered and (b) odd-membered poly(ester-imide)s

was calculated from the layer distances plotted in *Figure 12*. The assumption of an extended spacer being reasonable will be discussed in a future publication. The smaller tilt angle of mesogens in the odd-membered series has the consequence of a less stable crystal lattice, and thus of lower melting points. In other words the different tilt angles of the mesogens are responsible for the odd–even effect of T_{m_1} and T_{m_2} (*Figure 8*).

ACKNOWLEDGEMENT

We wish to thank the DAAD and Acciones Integrades for financial support and S. Buchner for calculating the tilt angles.

REFERENCES

1 De Abajo, J., de la Campa, J., Kricheldorf, H. R. and Schwarz, G. *Makromol. Chem.* 1990, **191**, 537
2 Kricheldorf, H., Schwarz, G. and Nowatzky, W. *Polymer* 1989, **30**, 936
3 Culbertson, B. M. US Patent 3 542 731 (1970) to Ashland Oil Co.; *Chem. Abstr. USA* 1971, **74**, 55430n
4 Kurita, K. and Matsuda, S. *Makromol. Chem.* 1983, **184**, 1223
5 Elsner, G., Riekel, C. and Zachmann, H. G. *Adv. Polym. Sci., Phys. Edn.* 1982, **20**, 719
6 Kricheldorf, H. R. and Pakull, R. *Macromolecules* 1988, **21**, 551